

A New High-Gain and Low-Complexity Pattern-Reconfigurable Antenna

Stylianos D. Assimonis^{1,2}, Argiris Theopoulos¹, Theodoros Samaras¹

¹ Dept. of Physics, Aristotle University of Thessaloniki, Greece

² School of ECE, Technical University of Crete, Chania, Greece

assimonis@physics.auth.gr, atheo@physics.auth.gr, theosama@auth.gr

Abstract—A new pattern-reconfigurable antenna, which operates from 2.36 GHz to 2.55 GHz and has maximum directivity 7.2 dB at horizontal plane, is presented in this work. In contrast to prior art designs, there is no ground plane, which usually displaces the directivity main lobe from the horizontal plane. In this paper, the main-lobe elevation angle is zero. The antenna is an Electronically Steerable Parasitic Array Radiator (ESPAR) antenna, based on Yagi-Uda concept, and utilizes printed elements on low-cost FR-4: a bow-tie dipole (driven-element) was surrounded by eight bow-tie parasitic-elements. The latter, which can be open or short-circuited using voltage-control RF switchers, act as directors or reflectors and hence accurately control the radiation pattern. The antenna was analyzed in terms of reflection coefficient and directivity and finally was fabricated and measured. Measurements agree well with simulations.

Index Terms—ESPAR antenna, beam steering, pattern-reconfigurable.

I. INTRODUCTION

In an urban environment a pattern-reconfigurable antenna with high directivity can be utilized in order to deal with the multi-path effect. In this direction, many designs have been proposed [1]–[5]. In [1] the antenna is able to provide three different radiation patterns using switchers on feeding network. In [2], pin RF-switchers were used and the antenna can steer the obtained radiation pattern. In [3], [4] the proposed designs adopted the Yagi-Uda antenna concept: a driven dipole radiates and adjacent parasitic-elements can be switched to directors or reflectors, accurately controlling the radiation pattern. However, in this case the main-lobe elevation angle is not zero due to the ground plane. In [5] an Electronically Steerable Parasitic Array Radiator (ESPAR) antenna using capacitive loading technique was presented. In order to reduce the geometry radius, authors used folded dipoles as parasitic elements, while in order to tune the direction of maximum radiation into horizontal plane, sleeve ground plane was one-quarter wavelength, leading to somewhat high height.

The goal of this work is to design and fabricate a low-cost and low-complexity pattern-reconfigurable antenna with high-directivity and zero main-beam elevation angle. In order to decrease the manufacturing cost, printed dipoles on low-cost but lossy FR-4 substrate was used, while in order to minimize the complexity, the Yagi-Uda antenna concept was adopted. Finally, it will be shown that the absence of ground plane leads the maximum directivity to appear on the horizontal plane.

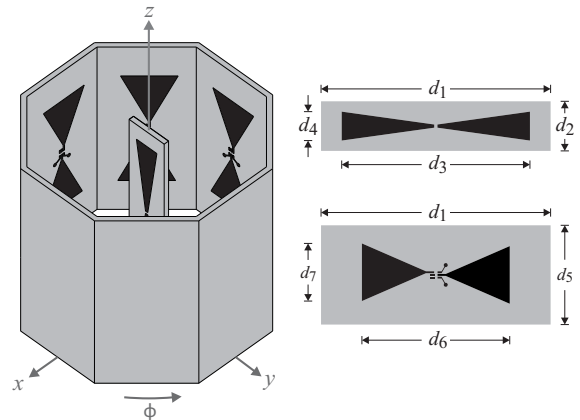


Fig. 1. The proposed antenna geometry (left): the driven-dipole (right, top) and one of the parasitic-dipoles (right, bottom).

TABLE I
THE OBTAINED OPTIMAL DIMENSIONS (MM).

d_1	d_2	d_3	d_4	d_5	d_6	d_7
55.56	2.08	45.56	0.90	25.27	35.79	13.95

II. ANTENNA DESIGN

A bow-tie antenna is an enhanced variation of a linear dipole antenna in terms of wide-band operation, without increasing the fabrication complexity [6]. In addition, the specific antenna resists small parameter fluctuations during manufacturing process. Finally, the existing gap between the two antenna arms can be used for easy RF switch mounting. Hence, the latter design was chosen: a printed bow-tie dipole (drive-antenna) was surrounded in a symmetric manner by eight printed bow-tie parasitic-elements (Fig. 1). The distance between driven and parasitic-elements is about $\lambda/4$. The substrate was low-cost and lossy FR-4 with $\epsilon_r = 4.55$, $\tan \delta = 0.01$ and thickness 1.5 mm. A voltage-control RF switch was placed between the two arms of each bow-tie and is manually controlled via a Double-Pole, Double-Throw (DPDT) DC switch. Hence the parasitic-elements can be open or short-circuited, acting as directors or reflectors, respectively, and finally, controlling the radiation pattern. The driven element is powered by a 50 Ohm coaxial cable, which is terminated with an SMA connector.

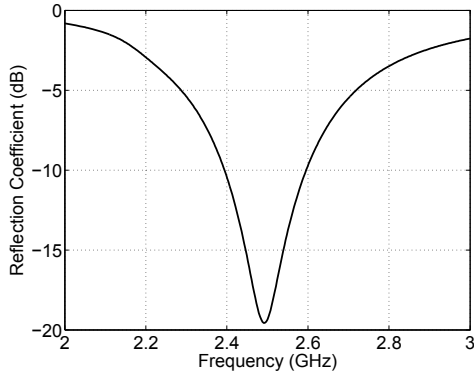


Fig. 2. Reflection coefficient when only one parasitic-element is short-circuited, located at $\phi = 0^\circ$: antenna operates from 2.39 to 2.59 GHz.

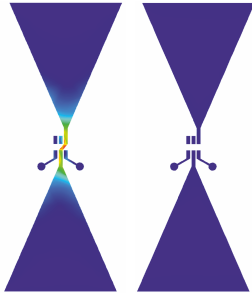
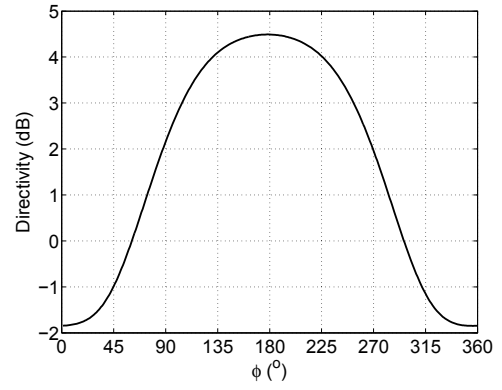


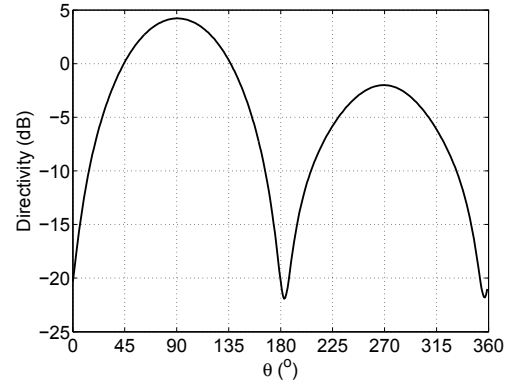
Fig. 3. Surface current distribution magnitude: on the short-circuited element (left) the current is much greater than that lies on the open-circuited (right) element, which is located on $\phi = 180^\circ$.

For simulations, Ansys HFSS (ANSYS Inc., Canonsburg, PA, USA) software was used. Second order vector finite elements have been implemented, while the computational domain is terminated with Perfectly Matched Layer (PML). All the metallic parts were treated as Perfect Electric Conductors (PEC), while, for excitation, a lumped port was applied to the driven element. The switching was modeled with gaps or PEC pads, which were placed between the two arms of each bow-tie: in open-circuited case a gap was introduced, while in short-circuited case the gap was filled with a metal pad. Optimization via genetic algorithm was applied during the design process. The goal was the minimization of the reflection coefficient for the band of 2.4 GHz to 2.5 GHz with only one parasitic-element short-circuited (“case 1”), located at $\phi = 0^\circ$. The obtained optimal dimensions are presented on Table I. Fig. 2 depicts the results: the antenna operates from 2.39 GHz to 2.59 GHz with a Fractional Bandwidth (FBW) 8%.

Fig. 3 depicts the surface current distribution magnitude of the only one short-circuited parasitic-element (left) in contrast to the surface current one of the open-circuited parasitic-element (right), which is located on $\phi = 180^\circ$, i.e. towards the maximum directivity. It is evident that the current on the short-circuited element is much greater than that on the open-circuited element, thus the short-circuited dipole acts as a reflector and steering the directivity main lobe to the opposite direction.



(a) Horizontal plane ($\theta = 90^\circ$)



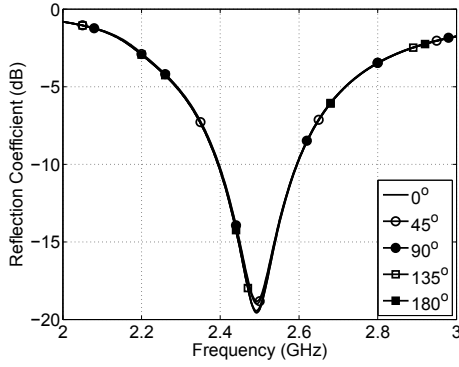
(b) Vertical ($\phi = 180^\circ$)

Fig. 4. Directivity at horizontal (a) and vertical (b) plane, respectively, when only one parasitic-element is short-circuited, located at $\phi = 0^\circ$. It is evident that the maximum lobe, with amplitude 4.5 dB, is located at horizontal plane.

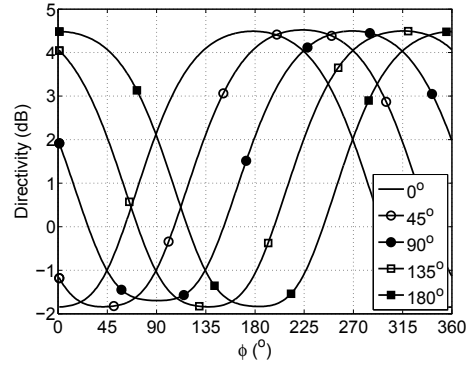
Fig. 4 illustrates the directivity at horizontal ($\theta = 90^\circ$) and vertical ($\phi = 180^\circ$) plane, respectively. It is shown that, maximum directivity (4.5 dB) occurs at horizontal plane and thus, elevation angle is zero. Moreover, main lobe is located at $\phi = 180^\circ$, i.e. indeed short-circuited element at $\phi = 0^\circ$ acts as a reflector.

Similar results are obtained when the short-circuited element location was sequentially rotated $0^\circ, 45^\circ, \dots, 180^\circ$. It was observed that the reflection coefficient remained almost constant (Fig. 5a) due to antenna symmetry, while the maximum directivity was also rotated with the same manner (Fig. 5b). Consequently, the beam not only can be accurately controlled and rotated 360° , but also maximum directivity is localized at horizontal plane.

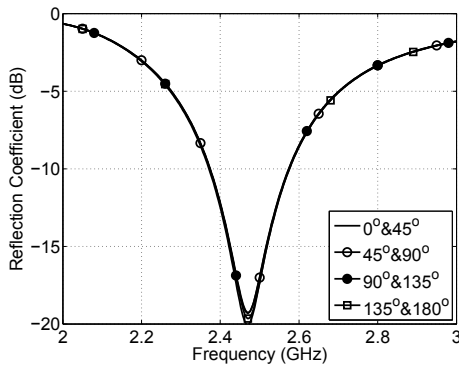
Next, multiple parasitic-elements were short-circuited and the obtained antenna was also analyzed in terms of reflection coefficient and radiation pattern. Fig. 5c, 5d depict the results when there are two shorted parasitic-elements (“case 2”), initially located at $\phi = 0^\circ$ and $\phi = 45^\circ$: the antenna operates from 2.37 to 2.57 GHz (i.e., FBW = 8.1%), while it has a maximum directivity of 6.26 dB at $\phi = 202.5^\circ$. Then, again, the short-circuited elements’ location was sequentially rotated $0^\circ, 45^\circ, \dots, 135^\circ$. It was also observed that, reflection



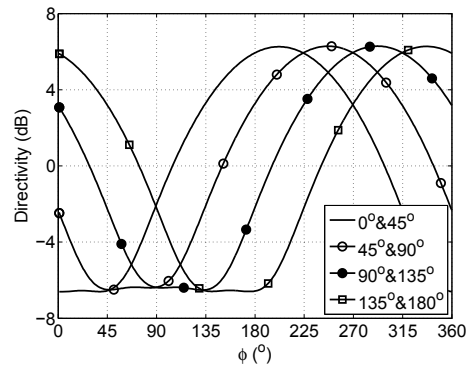
(a) Reflection coefficient: only one parasitic element is short-circuited, located at $\phi = 0^\circ, 45^\circ, \dots, 180^\circ$.



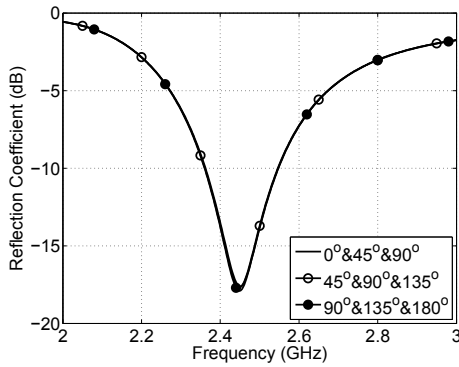
(b) Directivity: only one parasitic element is short-circuited, located at $\phi = 0^\circ, 45^\circ, \dots, 180^\circ$.



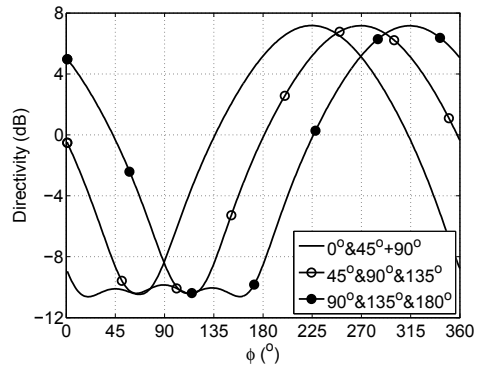
(c) Reflection coefficient: only two parasitic element are short-circuited, located at $0^\circ \& 45^\circ, 45^\circ \& 90^\circ, 90^\circ \& 135^\circ$ and $135^\circ \& 180^\circ$.



(d) Directivity: only two parasitic element are short-circuited, located at $0^\circ \& 45^\circ, 45^\circ \& 90^\circ, 90^\circ \& 135^\circ$ and $135^\circ \& 180^\circ$.



(e) Reflection coefficient: only three parasitic element are short-circuited, located at $0^\circ \& 45^\circ \& 90^\circ, 45^\circ \& 90^\circ \& 135^\circ$ and $90^\circ \& 135^\circ \& 180^\circ$.



(f) Directivity: only three parasitic element are short-circuited, located at $0^\circ \& 45^\circ \& 90^\circ, 45^\circ \& 90^\circ \& 135^\circ$ and $90^\circ \& 135^\circ \& 180^\circ$.

Fig. 5. The reflection coefficient (left) and directivity (right) for various number of short-circuited parasitic elements.

coefficient did not vary (Fig. 5c), while maximum directivity was also rotated with the same manner (Fig. 5d). Thereafter, three parasitic-elements were short-circuited (“case 3”) and the obtained antenna was also analyzed in terms of reflection coefficient and radiation pattern. According to simulations (Fig. 5e, 5f), the antenna operates from 2.36 to 2.55 GHz and has a FBW of 7.74%, while the directivity main lobe

is located at $\phi = 225^\circ$ and has a maximum amplitude of 7.2 dB. Hence, it is observed that, when the number of the shorted parasitic-elements is increased the maximum directivity is also increased. Finally, short-circuited elements were sequentially rotated $0^\circ, 45^\circ, 90^\circ$. Reflection coefficient remained almost constant once again (Fig. 5f), while the directivity was also rotated in the same manner (Fig. 5f).

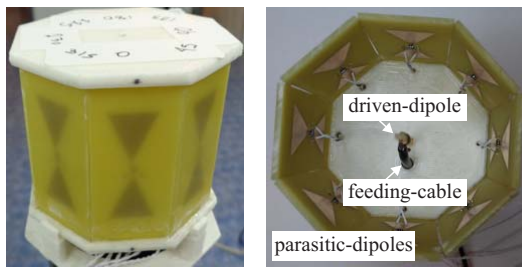


Fig. 6. The fabricated antenna: perspective (left) and top (right) view.

III. FABRICATION AND MEASUREMENT

In order to verify the simulation results, the antenna was fabricated using standard photo-lithographic techniques on a low-cost FR-4 substrate (Fig. 6). For switching, voltage-control switchers “AS179-92LF” (Skyworks Solutions, Inc.) were used. According to their datasheet, pin-J1 and -J3 were connected between the two arms of each parasitic-element, while pin-V1 and -V2 were connected to a control panel.

Initially, the fabricated antenna reflection coefficient was measured, by using a vector network analyzer, and the results are depicted in Fig. 7. For the sake of simplicity and due to the fact that this case results in the highest directivity, only one case is presented (“case 3”), with the three short-circuited parasitic elements located at $\phi = 0^\circ$, 45° and 90° , respectively. First, the agreement between the simulated and measured data is acceptable, although small discrepancies are observed. In particular, there is a difference between simulated and measured antenna bandwidth: according to measurement antenna operates from 2.41 to 2.5 GHz, thus has a FBW of 3.67%. This is probably due to the value used in the simulations for the dielectric constant of FR-4, the non-ideal behavior of the switchers (i.e., the isolation and the insertion losses are not perfect and zero, respectively), the driven-element feeding (i.e., the feeding coaxial cable is adjacent to the driven-dipole (Fig. 6) and finally, the influence of parasitic-elements weldings.

Next, the radiation pattern in terms of normalized directivity was tested. A log-periodic antenna was placed at “point a” and connected to a signal generator, transmitting a signal at 2.45 GHz. At far-field distance (“point b”), the proposed antenna was placed. The latter, which was rotatable with step 10° , was connected to a spectrum analyzer and the received power was measured. The simulated/measured normalized directivity is depicted in Fig. 8. Again only “case 3” (short-circuited parasitic elements located at $\phi = 0^\circ$, 45° and 90°) is presented here: a very good agreement is observed, while the measured front-to-back ratio is 20.8 dB.

IV. CONCLUSION

A new, high-directivity and low-complexity pattern-reconfigurable antenna, operating in the WiFi-band, was presented in this work. The design is based on the Yagi-Uda antenna concept: a driven dipole radiates and adjacent parasitic-elements can be switched to directors or reflectors, accurately

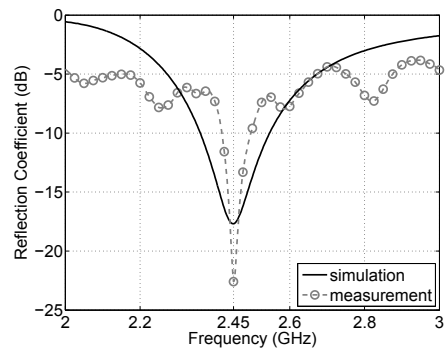


Fig. 7. The simulated/measured reflection coefficient for “case 3”.

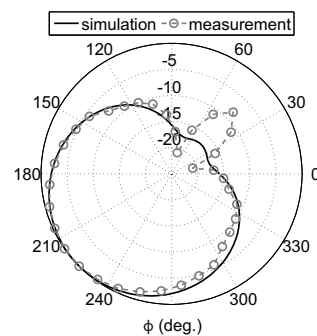


Fig. 8. The simulated/measured directivity for “case 3”.

controlling the radiation pattern. In contrast to prior art designs, there is no ground plane, which usually displace the directivity main lobe from the horizontal plane. The antenna was analyzed in terms of reflection coefficient and directivity and finally was fabricated and measured. Measurements agree well with simulations.

V. ACKNOWLEDGMENT

The research was financially supported by the “AQUANET” project (no. 11SYN_6_925), which is supported by the European Regional Development Fund and Greek National Funds.

REFERENCES

- [1] G.-M. Zhang, J.-S. Hong, B.-Z. Wang, G. Song, and P. Li, “Design and time-domain analysis for a novel pattern reconfigurable antenna,” *IEEE Antennas Wireless Propag. Lett.*, vol. 10, pp. 365–368, 2011.
- [2] S. Nikolaou, R. Bairavasubramanian, C. Lugo, I. Carrasquillo, D. Thompson, G. E. Ponchak, J. Papapolymerou, and M. M. Tentzeris, “Pattern and frequency reconfigurable annular slot antenna using PIN diodes,” *IEEE Trans. Antennas Propag.*, vol. 54, no. 2, pp. 439–448, 2006.
- [3] R. Schlub, J. Lu, and T. Ohira, “Seven-element ground skirt monopole ESPAR antenna design from a genetic algorithm and the finite element method,” *IEEE Trans. Antennas Propag.*, vol. 51, no. 11, pp. 3033–3039, 2003.
- [4] Z. Shi, R. Zheng, J. Ding, and C. Guo, “A novel pattern-reconfigurable antenna using switched printed elements,” *IEEE Antennas Wireless Propag. Lett.*, vol. 11, pp. 1100–1103, 2012.
- [5] H.-T. Liu, S. Gao, and T.-H. Loh, “Electrically small and low cost smart antenna for wireless communication,” *IEEE Trans. Antennas Propag.*, vol. 60, no. 3, pp. 1540–1549, 2012.
- [6] C. A. Balanis, *Antenna theory: analysis and design*. John Wiley & Sons, 2012.